# A robust method for quantifying the contribution of transient dynamics to variation in population growth rate

Christina M. Hernández*[1,†], Harman Jaggi[2,†], James Cant[1, +], Wenyun Zuo[3], Shripad Tuljapurkar[3,‡], and Roberto Salguero-Gómez[1, ‡]

[1]University of Oxford, Department of Biology, South Parks Road, Oxford OX1 3RB, UK
[2]Princeton University, Ecology and Evolutionary Biology, NJ, 08540, USA
[3]Stanford University, Department of Biology, CA, 94305, USA
[†]Co-first-authors; These authors contributed equally.
[‡]Co-senior-authors; These authors contributed equally.
[+]Present address: Centro de Ciências do Mar e do Ambiente (MARE), Faculdade de Ciências, Universidade de Lisboa, Lisboa, Portugal.

August 21, 2026

A manuscript for preprinting at EcoEvoRxiv before peer review

**Running title** Decomposing variance in population growth

**Acknowledgements** This work was supported by a NERC Pushing the Frontiers grant (NE/X013766/1) to RSG. CMH was additionally supported by a Marie Curie Fellowship [MSCA DensPopDy #10115386] with funding through UKRI [grant number EP/Z002826/1], hosted by RSG. ST, HJ and WZ were not supported by any government funding sources.

**Author Contributions** All authors conceived of the project. HJ, WZ, and ST derived the mathematical expressions and analytical insights. CMH wrote functions and code with input from RSG and ST. CMH selected and analyzed the case studies and made the figures. CMH and HJ wrote the first draft of the manuscript, and all authors revised the manuscript.

**Data availability statement** The data that support the findings of this study are openly available at www.compadre-db.org. All code files required to repeat the analyses are archived at Zenodo (https://doi.org/10.5281/zenodo.19093535).

**Word count** Abstract: 234, Main text: 5963
**Figures** Main text: 2 figures, 2 tables

*Corresponding author. Present address: Department of Biological Sciences, Old Dominion University, Norfolk, Virginia, USA. Email: cmhernan@odu.edu

# Abstract

Understanding why population growth rates vary through time is central to ecology, evolution, and conservation. In structured populations, such variation arises from both environmentally-driven fluctuations in vital rates and the resultant transient fluctuations in population structure. Despite long-standing recognition of these processes, existing approaches do not provide an exact and general partitioning of their relative contributions. Here, we build on stochastic population theory to develop a mathematically rigorous framework that decomposes variation in realized population growth rate into contributions from fluctuations in vital rates, fluctuations in population structure, and their interaction. Additionally, we develop analytical expressions for the first-order variance contributions associated with vital rates vs. population structure. This framework clarifies how damping rate, life-history speed, and covariance among vital rates shape temporal variability in growth. We complement the analytical results with a simulation-based procedure that calculates the decomposition from time series of population projection matrices without requiring observations of past population structure. Applying the methods to empirical case studies spanning plants and animals with contrasting generation times, we show that short-lived species exhibit variability dominated by vital-rate fluctuations, whereas long-lived species can exhibit substantial contributions from transient population structure when vital-rate variation is sufficiently large. Our approach provides a unifying and exact link between stochastic demography and transient dynamics, offering a powerful tool for comparing life histories, testing ecological hypotheses, and evaluating how environmental variability propagates through population structure to influence population growth.

**Data/code for peer review statement:** An anonymized version of the code has been provided as a zip file containing five (5) R script files. We have also provided an anonymized README.txt file, and two CSV data files. The data files are not needed to run our code, but provide information about the populations that were available for selection as case studies.



**Keywords:** convergence, matrix population models, population structure, stochastic demography, short-term dynamics, variance decomposition.

# 1 Introduction

Population growth rate underpins many ecological and evolutionary processes, with key implications for the conservation of wild populations (Sibly and Hone, 2002). For instance, population growth rate is often considered a proxy measure for the average fitness of a population (Crone et al., 2011; Metz et al., 1992), and invasion growth rates are commonly used to understand coexistence (Godoy and Levine, 2014). Ecosystem management efforts, both in terms of conservation (Hone et al., 2010) and pest management (Thomas, 1999) also focus on setting population growth rate to a target level (Koons et al., 2006; Sutherland and Norris, 2002). As such, an important and long-standing question is: what factors drive variation in population growth rate?

In demographic models, variation in population growth rate can be generated by both extrinsic and intrinsic dynamics. In these models, individuals are structured by age, size, and/or stage (simply "stage" hereafter), according to how an individual's stage affects their probability of survival or reproductive output (Caswell, 2001; Ellner et al., 2016). By extrinsic dynamics, we refer to the possible ways that survival, growth, and reproduction can be impacted by temporal variation in the environment—this could be related to abiotic (*e.g.*, Lindell et al., 2022; Oldfather and Ackerly, 2019; Paniw et al., 2021) or biotic (*e.g.*, Greenberg and Green, 2013; Rudgers and Hoeksema, 2003) factors. By intrinsic dynamics, we refer to the fact that variation in population structure can generate fluctuations in population growth rate, even if vital rates are constant (Stott et al., 2011). These mechanisms whereby a structured population model generates fluctuations in growth rate, and the study of these processes and their consequences, obviously involve non-steady, *i.e.* transient, dynamics (Hastings, 2004; Jaggi et al., 2026b; Stott et al., 2011).

In a structured population model, these intrinsic and extrinsic drivers are linked to one another through the population structure, the proportional distribution of the population stages. Many matrix population models for plants and animals use fixed vital rates and are ergodic, meaning that their long-term behavior is independent of their initial conditions (Stott et al., 2010; Tuljapurkar, 1990). In such cases, population size would eventually grow or shrink at a constant exponential rate (Caswell, 2001, page 79-92). From then on, the population structure would also remain constant while population size increases or declines.

However, when (a)biotic conditions—and, as a consequence, vital rates—change across time, the population growth rate varies from year to year without converging to a constant value. When variability is statistically similar over the years, i.e., statistically stationary, a stochastic ergodicity replaces the classical ergodicity (Tuljapurkar, 1990). In such cases, the population structure does change from year to year, but has an unchanging probability distribution.

Temporal variation in population growth rate can be separated into contributions from two sources (Tuljapurkar, 1990). The first, and more obvious source, is the immediate effect that changes in the environment have on changes in vital rates of survival, growth, and fecundity. For instance, in a bad year for reproduction, population growth rate will tend to be lower than in a year that is good for reproduction. The second, perhaps less obvious source, is the effect of the population structure on population growth rate. For example, if population structure is concentrated in non-reproductive classes, then the (one-step-ahead) population growth rate will tend to be lower than if the population structure were concentrated in reproductive classes. When vital rates vary through time, the population structure also varies—low reproductive output at time 1 will lead to a low relative frequency of young individuals at time 2. Therefore, the population structure at a specific time results from the accumulated effects of a population's history of variation in vital rates. Moreover, that variation in population structure has its own effect on realized population growth rate independent of any vital rate effects[1] (Hastings et al., 2018; McDonald et al., 2016). So an important question is the relative importance of vital rates and population structure in driving variation in population growth rate.

Demographers have developed a rich toolbox of methods for analyzing variation in population growth rate for structured population models. For example, sensitivity and elasticity analyses quantify the effect on population growth rate of changes in vital rates (De Kroon et al., 2000; Heppell et al., 2000). Said metrics can be applied to models that are deterministic (Caswell, 2007; Caswell, 2019) or stochastic (Haridas and Tuljapurkar, 2005; Kajin et al., 2025; Tuljapurkar et al., 2003). Life Table Response Experiments (LTREs) decompose the deviance or variance in population growth rate between/among empirical population models into the contributions from various vital rates (Caswell, 1989; Hernández et al., 2023; Knape et al., 2023; Koons et al., 2016). However, none of these approaches allow us to distinguish be-

[1] Assuming that variation in vital rates is independent of population density.

tween the effect of immediate changes in vital rates from the accumulated effects of historical variation in vital rates. If we had a complete time series of vital rates, population structure, and realized population growth rate (Koons et al., 2016), we could use the transient LTRE method for decomposing the variance in population growth rate into contributions from vital rates and population structure. In practice, the data requirements have thus far limited the application of transient LTRE (but see Dobson et al. 2024; Knape et al. 2023; Maldonado-Chaparro et al. 2018; Summers et al. 2024). In contrast, stochastic population theory is based on a view of environmental variation wherein repeated observations of vital rates are samples from a stationary noisy process that may or may not include autocorrelation (Jaggi et al., 2024a; Jaggi et al., 2026a; Robey et al., 2025; Tuljapurkar and Haridas, 2006).

Here, we focus on this stochastic view of the environmentally-driven variation in vital rates. In this view, we can assume that temporally-replicated observations of vital rates (*e.g.*, matrix population models) are random samples from a stationary distribution of vital rate combinations arising from different environmental states. Based on this same framework of stochastic variation in vital rates, past research used correlation approaches to decompose variation in population growth rate, showing that the contributions from variation in population structure is important in plants (Ellis and Crone, 2013; McDonald et al., 2016). However, the decomposition that those works employ (Equation 2 in Ellis and Crone 2013) relies only on the projection matrix and population structure at a particular time. Therefore, those methods cannot separate the variation in growth rate over time into the contributions of vital rates and population structures. Here, instead, we present and implement a mathematically complete and exact decomposition of population growth rate into contributions from vital rates and contributions from population structure. Our work follows the approach in Tuljapurkar (1990).

We first introduce the mathematical decomposition of variance in realized population growth rate. Next, we discuss several analytical insights that emerge from the approach. Then, we detail how to use a timeseries of matrix models to calculate the contribution terms using both the analytical expressions and a simulation-based decomposition. Finally, we explore a few case studies to demonstrate the ecological interpretation of results and whether they match the analytical expectations.

Table 1: Notation and definitions. Some operators are provided in the first block, and then variables are listed below. We employ the convention for matrix mathematics (following Caswell 2001 and others) wherein vectors are named with lower-case boldface English letters, and matrices are named with upper-case boldface English letters.

| Notation | Formula and/or meaning |
|---|---|
| | **Operators** |
| $\mathbf{e}$ | A vector where all entries are 1. |
| $(\mathbf{x}, \mathbf{y})$ | The inner product of vectors $\mathbf{x}$ and $\mathbf{y}$. |
| $(\mathbf{e}, \mathbf{x})$ | The inner product of $\mathbf{e}$ and $\mathbf{x}$ is equivalent to the sum of the entries in the vector $\mathbf{x}$. |
| $\mathcal{E}[X]$ | Expected value or time-averaged value of $X$. |
| | **Other parameters and variables** |
| $\mathbf{A}_t$ | The population projection matrix containing the vital rates experienced by the focal population from time $t-1$ to time $t$. |
| $\overline{\mathbf{A}}$ | The population projection matrix long-term mean vital rates experienced by the focal population. |
| $\mathbf{H}_t$ | The matrix of random deviations to the entries of $\overline{\mathbf{A}}$ that give rise to $\mathbf{A}_t$. |
| $\mathbf{w}_t$ | The population structure vector at time t. |
| $\overline{\mathbf{w}}$ | Long-term average population structure vector. |
| $\mathbf{z}_t$ | Vector of deviations between $\mathbf{w}_t$ and $\overline{\mathbf{w}}$. |
| $\lambda_t$ | Population growth rate from time $t-1$ to time $t$. |
| $\overline{\lambda}$ | Long-term average population growth rate. |
| $\lambda_d$ | Deterministic population growth rate of a population growing according to $\overline{\mathbf{A}}$, calculated as the leading eigenvalue of $\overline{\mathbf{A}}$. |
| $\Delta_Z$ | Contribution to $\lambda_t$ from the mean vital rates acting on the deviation in population structure, defined as $\left(\mathbf{e}, \overline{\mathbf{A}}\mathbf{z}_{t-1}\right)$. |
| $\Delta_R$ | Contribution to $\lambda_t$ from the deviations in vital rates acting on the mean population structure, defined as $(\mathbf{e}, \mathbf{H}_t\overline{\mathbf{w}})$. |
| $\Delta_{ZR}$ | Contribution to $\lambda_t$ from the deviations in vital rates acting on the deviation in population structure, defined as $(\mathbf{e}, \mathbf{H}_t\mathbf{z}_{t-1})$. |
| $\epsilon$ | Scaling parameter representing the size of the deviations to $\overline{\mathbf{w}}$ and $\overline{\mathbf{A}}$. |

# 2 Methods

In this section, we introduce the time-varying population model and the decomposition of the population growth rate into the effects of changes in vital rates and population structure. To understand the influence of fluctuations in vital rates and population structure on population growth rate, we decompose the variance in population growth rates into contributions from variance in vital rates and variance in population structure. We then derive analytical expressions for those contribution terms and discuss the implications of those analytical results. Finally, we present a simulation approach to compute the decomposition for any time series of matrix population models. Our notation is summarized in Table 1.

## 2.1 Population model

We assume that we have a sequence of population projection matrices ($\mathbf{A}_t$), each representing the vital rates applying to the transition between a subsequent pair of annual censuses. The time-varying projection matrix $\mathbf{A}_t$ can be expressed as:

$$\mathbf{A}_t = \overline{\mathbf{A}} + \mathbf{H}_t, \text{ with } \mathcal{E}[\mathbf{H}_t] = 0. \tag{1}$$

Here, we have decomposed (as we always may) the matrix $\mathbf{A}_t$ at time $t$ into $\overline{\mathbf{A}}$, the mean projection matrix, and $\mathbf{H}_t$ the perturbation matrix. Each element $h_{ij,t}$ represents the deviation at time $t$ from the mean value of the corresponding element in $\overline{\mathbf{A}}$. The symbol $\mathcal{E}$ represents a time average a long finite interval or an expectation over a distribution.

By definition, the expected values (*i.e.*, the average over time) of the perturbations must be equal to 0, or else they would cause the entries of the mean matrix to change. The dominant eigenvalue of the average matrix $\overline{\mathbf{A}}$ is called $\lambda_d$, with corresponding normalized right eigenvector $\mathbf{u}$.

Let $\mathbf{w}_t$ denote the population structure at time $t$. The projection matrix $\mathbf{A}_t$ applies between $t-1$ and $t$, and maps the stage structure at the beginning of the time interval $(t-1, t)$ to $\mathbf{w}_t$. The population structure is expressed as the proportion of individuals in each class, so the structure always sums to 1, *i.e.*, $(\mathbf{e}, \mathbf{w}_t) = 1$, where $\mathbf{e}$ is a vector of ones and $(\cdot, \cdot)$ indicates a scalar product between two vectors.

We refer to the realized population growth rate from time $t-1$ to time $t$ as $\lambda_t$, the ratio of population size at time $t$ over population size at time $t-1$:

$$\lambda_t = \frac{(\mathbf{e}, \mathbf{A}_t\, \mathbf{w}_{t-1})}{(\mathbf{e}, \mathbf{w}_{t-1})} = (\mathbf{e}, \mathbf{A}_t \mathbf{w}_{t-1}). \tag{2}$$

The population structure at time $t$ is given by

$$\mathbf{w}_t = \frac{\mathbf{A}_t\, \mathbf{w}_{t-1}}{\lambda_t} = \overline{\mathbf{w}} + \mathbf{z}_t. \tag{3}$$

Just as we decomposed the projection matrix ($\mathbf{A}_t$), we express the population structure $\mathbf{w}_t$ as the sum of mean and perturbation components, where $\overline{\mathbf{w}}$ is the average (long-term) stage distribution and $\mathbf{z}_t$ is the deviation of the population structure from $\overline{\mathbf{w}}$ at time $t$. Because

stage structure is expressed as proportions, the sum of the deviations of the structure must sum to 0 (an increase in one stage class relative to $\overline{\mathbf{w}}$ must be balanced by a decrease in another stage class), hence $(\mathbf{e}, \mathbf{z}_t) = 0$.

## 2.2 Decomposing realized population growth rate

In structured populations, changes in abundance over time can be influenced by (1) how individuals are distributed across stages, and (2) how vital rates (survival, growth, reproduction) vary over time. To separate these effects, we combine the expression for realized population growth rate (Equation (2)) with the expressions for the projection matrix (Equation (1)) and population structure (Equation (3)). This allows us to decompose realized population growth rate into contributions from the mean long-run growth rate, fluctuations in population structure, fluctuations in vital rates, and their interaction. The population growth rate can be expanded as follows:

$$\begin{aligned}
\lambda_t &= (\mathbf{e}, \mathbf{A}_t \mathbf{w}_{t-1}) \\
&= \big(\mathbf{e}, (\overline{\mathbf{A}} + \mathbf{H}_t)(\overline{\mathbf{w}} + \mathbf{z}_{t-1})\big) \\
&= (\mathbf{e}, \overline{\mathbf{A}}\overline{\mathbf{w}}) + (\mathbf{e}, \overline{\mathbf{A}}\mathbf{z}_{t-1}) + (\mathbf{e}, \mathbf{H}_t\overline{\mathbf{w}}) + (\mathbf{e}, \mathbf{H}_t\mathbf{z}_{t-1}) \\
&= \boxed{\overline{\lambda} + \Delta_Z + \Delta_R + \Delta_{ZR}}
\end{aligned} \tag{4}$$

where

- $\overline{\lambda}$ is the time-averaged population growth rate. When the variability in vital rates over time is small, the average growth rate is simply the dominant eigenvalue of the mean projection matrix $\overline{\mathbf{A}}$,
- $\Delta_Z = (\mathbf{e}, \overline{\mathbf{A}}\mathbf{z}_{t-1})$ represents the effect on population growth rate from fluctuations in population structure when mean vital rates are applied,
- $\Delta_R = (\mathbf{e}, \mathbf{A}_t\overline{\mathbf{w}})$ represents the effect of fluctuations in vital rates acting on the mean population structure, and
- $\Delta_{ZR} = (\mathbf{e}, \mathbf{H}_t\mathbf{z}_{t-1})$ represents the effect of fluctuations in vital rates acting on fluctuations in population structure (the interaction term).

Ecologically, this means that deviations in the one-step-ahead population growth rate $\lambda_t$ from the long-term mean growth rate $\overline{\lambda}$ can occur either because the population structure is away from its stable state distribution, because of variability in vital rates such as survival or reproduction, or because of an interaction between these.

## 2.3 Decomposition of variance in $\lambda_t$

Here we decompose the *variance* in population growth rate into contributions from fluctuations in population structure, vital rates, and their interactions. Using Equation (4), we find:

$$\begin{aligned} \mathrm{Var}\lambda_t = &\boxed{\mathrm{Var}(\Delta_Z) + \mathrm{Var}(\Delta_R)} + 2\,\mathrm{Cov}(\Delta_Z, \Delta_R) + \\ &+ 2\,[\mathrm{Cov}(\Delta_Z, \Delta_{ZR}) + \mathrm{Cov}(\Delta_R, \Delta_{ZR})] + \mathrm{Var}(\Delta_{ZR}). \end{aligned} \tag{5}$$

For most applications of this decomposition, we expect variance in population growth rate to be dominated by the first two terms of this decomposition (the boxed portion of Equation (5)). Firstly, this is true if fluctuations tend to be small (see Section 2.4 below). Secondly, if the fluctuations in population structure and vital rates are uncorrelated (*e.g.* systems without temporal environmental autocorrelation and without density-dependent feedbacks), then their covariance should be 0. However, our simulation procedure described in Section 3.2 does not rely on these assumptions and the code we provide enables the full decomposition including all six terms.

The first term $\mathrm{Var}(\Delta_Z)$ corresponds to variance due to deviations in population structure from its average stage distribution ($\overline{\mathbf{w}}$). Because these deviations are generated by past fluctuations in vital rates, this term reflects how much demographic memory (*sensu* Jaggi et al. 2026b; Tuljapurkar and Haridas 2006) the system has. More specifically, this term reflects the importance of transient dynamics—how responsive the system is to fluctuations and how quickly those responses decay. The second term $\mathrm{Var}(\Delta_R)$ corresponds to variance generated by fluctuations in the vital rates. Since this term depends on the random perturbation matrix $\mathbf{H}_t$ acting on the mean population structure $\overline{\mathbf{w}}$, $\mathrm{Var}(\Delta_R)$ captures the effect of variability in survival, growth, or reproduction at time $t$, independent of transient effects of population

structure. Together, these terms describe how variation arises both from extrinsic variation in vital rates and from intrinsic demographic memory.

## 2.4 Analytical results to generate ecological expectations

To generate ecological expectations about how model components drive the variance terms, we adopted the assumptions of small fluctuations and no covariance. From these assumptions, we developed analytical expressions for the variance of main effects, $\mathrm{Var}(\Delta_Z)$ and $\mathrm{Var}(\Delta_R)$, the terms that we expect to dominate the decomposition (Equation (5)). Here, we introduce the assumptions, the analytical results, and their ecological implications; in Appendices S2-S5, we provide the full derivations of the analytical expressions.

The size of fluctuations is measured by their coefficient of variation, for which we use the parameter $\epsilon$. In that case, Equation 1 is replaced by

$$\mathbf{A}_t = \overline{\mathbf{A}} + \epsilon\,\mathbf{H}_t, \text{ with } \mathcal{E}[\mathbf{H}_t] = 0. \tag{6}$$

The dominant eigenvalue of $\overline{\mathbf{A}}$ is $\lambda_d$, with the corresponding right eigenvector $\mathbf{u}$ (the stable population structure). Equation 2 is replaced by

$$\mathbf{w}_t = \mathbf{u} + \epsilon\,\mathbf{z}_t, \tag{7}$$

and Equation (4) is replaced by

$$\lambda_t = \boxed{\lambda_d + \epsilon\Delta_Z + \epsilon\Delta_R + \epsilon^2\Delta_{ZR}}. \tag{8}$$

Using these, the variance decomposition Equation 6 is replaced by (in increasing order of $\epsilon$):

$$\begin{aligned}\mathrm{Var}\lambda_t = &\boxed{\epsilon^2\mathrm{Var}(\Delta_Z) + \epsilon^2\mathrm{Var}(\Delta_R)} + \epsilon^2\,2\,\mathrm{Cov}(\Delta_Z, \Delta_R) + \\ &+ \epsilon^3\,2\,[\mathrm{Cov}(\Delta_Z, \Delta_{ZR}) + \mathrm{Cov}(\Delta_R, \Delta_{ZR})] + \epsilon^4\,\mathrm{Var}(\Delta_{ZR}).\end{aligned} \tag{9}$$

Because we assume small fluctuations (small $\epsilon$) and no covariance, all but the boxed terms become vanishingly small. These assumptions furthermore lead us to analytical expressions for the two terms that remain dominant, $\mathrm{Var}(\Delta_Z)$ and $\mathrm{Var}(\Delta_R)$.

First, our analytical results imply that the *contribution from variance in vital rates*, $\mathrm{Var}(\Delta_R)$, depends on how the life history of the population interacts with environmental variation. Mathematically, the contribution from variance in vital rates is given by the product of the variance-covariance matrix of vital rate perturbations ($\mathcal{E}[\mathbf{H}_t \otimes \mathbf{H}_t]$) and the stable population structure ($\mathbf{u}$):

$$\mathrm{Var}(\Delta_R) = \left(\mathbf{e}^T \otimes \mathbf{e}^T\right)\, \mathcal{E}[\mathbf{H}_t \otimes \mathbf{H}_t]\, (\mathbf{u} \otimes \mathbf{u})\,. \tag{10}$$

In other words, the contribution from variance in vital rates is the sum of the variance in vital rates, weighted by the stable distribution. Ecologically, this means that the contributions of fluctuations in vital rates will be highest if there is high variance in vital rates corresponding to stages that are prevalent in the stable stage distribution. For example, if germination rate is highly variable and the population structure is strongly skewed towards seeds, then we would see a high contribution from $\Delta_R$.

In the case of the *contribution from variance in population structure*, $\mathrm{Var}(\Delta_Z)$, the story is a little bit more complicated. Mathematically, this contribution term is proportional to the product of the mean vital rates ($\overline{\mathbf{A}}$) and the variance-covariance matrix of fluctuations in population structure ($\mathcal{E}[\mathbf{z}_t \otimes \mathbf{z}_t]$):

$$\mathrm{Var}(\Delta_Z) = \left(\mathbf{e}^T \otimes \mathbf{e}^T\right)\, \left(\overline{\mathbf{A}} \otimes \overline{\mathbf{A}}\right) \mathcal{E}\left[\mathbf{z}_t \otimes \mathbf{z}_t\right] \tag{11}$$

The variance-covariance matrix of fluctuations in population structure is itself a product of the variance-covariance matrix of vital rates, the stable population structure, and the transient portion of the population matrix (Equation S52). Therefore, the contributions from variance in population structure will be highest in models where the transient dynamics decay slowly. Remember that, in our model, the variation in population structure is generated by the perturbations to vital rates that occurred in past time steps. So, populations with more excitable population structure or with more "memory" for these past vital rate perturbations will show a greater contribution from $\Delta_Z$. Because convergence rate is inversely proportional to generation time (Jiang et al., 2022), we would expect greater contributions from variance in population structure in long-lived and late-maturing species.

These analytical results also underscore the importance of covariances between vital rates

in driving the overall variance in population growth rate. Both variance contribution terms depend ultimately on the variance-covariance matrix of vital rate perturbations. Therefore, both contribution terms—and, by extension, overall variance in population growth rate—can be minimized if there are negative covariances between vital rates. If good years for survival are bad years for fecundity and *vice versa*, then the fluctuations in population growth rate will be small. The damping effect of these negative covariances among vital rates are mediated through both the contributions of variance in vital rates and the contributions of variance in population structure.

In light of these analytical results, we can make some predictions about which life history strategies should exhibit variation in population growth rate dominated by contributions from vital rates *vs.* contributions from structure. Species with a fast life history tend to have population structures skewed towards small, vulnerable stages and to exhibit higher variance in survival than reproduction. As such, we would expect them to exhibit relatively high variation in population growth rate with the contributions from vital rates dominating. Meanwhile, species with a slow life history tend to have populations with more even distributions across young and old individuals (but reproductive strategy can be important here, *e.g.*, fish and trees). Furthermore, species with long generation time should exhibit more "memory" of past vital rate perturbations, meaning that we expect their variation in population growth rate to be dominated by contributions from population structure.

# 3 Applying calculations to matrix population models

To implement our variance decomposition methods to understand how variation in population growth rate is driven by fluctuations in population structure *vs.* vital rates, users need a set of population projection matrices representing different times or environmental states. These can come from empirical measurements of population vital rates (*e.g.*, a time series of $\mathbf{A}_t$) or the combination of a mean matrix ($\overline{\mathbf{A}}$) and a time series of perturbation matrices ($\mathbf{H}_t$). In our case studies (Section 4), we use sets of projection matrices ($\mathbf{A}_t$) from the COMADRE (Salguero-Gómez et al., 2016) and COMPADRE (Salguero-Gómez et al., 2015) databases where there is temporal replication at the population level. Note that when we work with empirically-based projection matrices, we use $\epsilon = 1$.

### 3.1 Calculating the analytical terms

The analytical terms can be calculated directly from a set of projection matrices. For example, Equation (10) requires two objects that can be calculated from the set of $\mathbf{A}_t$ matrices: (1) the set of $\mathbf{H}_t$ matrices which are the deviations of each $\mathbf{A}_t$ from $\overline{\mathbf{A}}$, and (2) the stable population structure $\mathbf{u}$ which is the right eigenvector corresponding with the leading eigenvalue of $\overline{\mathbf{A}}$. Likewise, the analytical expression for $\mathrm{Var}(\Delta_Z)$ can be calculated using only the set of $\mathbf{A}_t$ matrices (11) (see Equation (S52) or our supplemental code to see how to calculate the variance-covariance matrix of fluctuations in population structure from the $\mathbf{A}_t$ matrices).

### 3.2 Using simulations to decompose growth rate

To numerically calculate the terms in the variance decomposition of population growth rate into the contributions shown in Equation (5), we use a simulation procedure. To characterize the variation in $\lambda_t$, we need a large number of replicate simulated population trajectories — we recommend at least 500. For each replicate trajectory, we generate a randomly-drawn time series of the $\mathbf{A}_t$ projection matrices. In this study, we assume no serial autocorrelation and that all matrices in the set have uniform likelihood of being drawn for each time step; however, users could adapt the simulation method to include autocorrelation in the environment or other probability distributions for the environmental conditions. For each replicate trajectory, we project the population forward from an initial population vector that is evenly distributed across classes. To remove any effects of this initial population vector, we use a burn-in period, *i.e.*, simulation time steps that are discarded before calculating the decomposition. We recommend a burn-in time of $100T_g$, where $T_g$ is the generation time. This period is sufficiently long to remove any effects of the initial population vector. The decomposition is then calculated for one time step following the burn-in.

For each replicate, we attain values for: (1) the projection matrix for the final time step ($\mathbf{A}_t$), (2) the population structure at the start of the final time step ($\mathbf{w}_{t-1}$) and (3) the realized population growth rate for the final time step ($\lambda_t = (\mathbf{e}, \mathbf{A}_t\mathbf{w}_{t-1})$).

From these three pieces of information ($\mathbf{A}_t$, $\mathbf{w}_{t-1}$, and $\lambda_t$), we are able to calculate the terms in Equation (4). Specifically, we calculate the mean matrix $\overline{\mathbf{A}}$ across all replicate values of $\mathbf{A}_t$, the mean population structure $\overline{\mathbf{w}}$ across all replicate values of $\mathbf{w}_{t-1}$, and then use these to calculate the $\Delta_Z$, $\Delta_R$, and $\Delta_{ZR}$ for each replicate. Finally, we calculate the terms of the

variance decomposition given in Equation (5) by taking the variances and covariances of the $\Delta$ terms across replicates.

For a more detailed explanation of our simulation algorithm, see Supplemental Section S6 or our supplemental code.

# 4 Case studies

To demonstrate the application of both our analytical and simulation methods, as well as interpretation of the results, we present several case studies. We selected these case studies from the COMADRE and COMPADRE databases of matrix population models from animals and plants, respectively (Salguero-Gómez et al., 2015; Salguero-Gómez et al., 2016). First, we filtered the 3,488 and 8,994 matrices in COMADRE (v4.23.2.1) and COMPADRE (v6.23.5.0), respectively, for matrices that represented natural populations under unmanipulated conditions. To focus on populations with the ability to exhibit transient dynamics, we excluded any studies where the life cycle was represented with fewer than three stages. We required that these matrices were separable into survival transitions among classes ($\mathbf{U}$ matrix), and reproduction ($\mathbf{F}$ matrix) so that we could calculate generation time using the definition of Bienvenu and Legendre (2015). We also required that sexual reproduction was observed/included in the study design, and we excluded models with clonal reproduction. We removed any matrices with impossible survival values, *i.e.*, any columns in the $\mathbf{U}$ matrix with a column sum greater than 1.001. We then restricted our subset to studies that contained at least four matrices for the same species. These selection criteria left us with 472 and 1,981 matrices from 29 and 144 species for animals and plants, respectively.

Next, we manually inspected these sets to identify groups of matrices that pertained to temporal replication at the same population or geographic site. Our manually-screened sets of matrices are given in the archived data files `comadre_ScreenedMatrixSets.csv` and `compadre_ScreenedMatrixSets.csv` for animals and plants, respectively. From those possible populations, we selected a few that cover a range of generation times, with preference for particularly long time series. The details of the populations we selected are given in Table 2 and each study is briefly introduced along with biological interpretation of the results.

We first illustrate the importance of incorporating population structure in the Appendix

Table 2: Information on case studies. All matrix population models have a time step of one year. Generation time ($T_g$) is measured in years. Population growth rate ($\lambda_d$) refers to the eigenvalue of the mean matrix $\overline{\mathbf{A}}$.

| **Species** | **Common name** | **Reference** | $T_g$ | **N matrices** | $\lambda_d$ |
|---|---|---|---|---|---|
| *Orcinus orca* | Orca | Vélez-Espino et al. (2014) | 32 | 24 | 0.989 |
| *Actaea spicata* | Baneberry | Fröborg and Eriksson (2003) | 17 | 6 | 0.975 |
| *Dicerandra frutescens* | Scrub mint | Menges et al. (2006) | 16 | 9 | 0.838 |
| *Callospermophilus lateralis* | Golden-mantled ground squirrel | Hostetler et al. (2012) | 1 | 18 | 2.05 |

figures S1. In our examples, we compare structured matrix population models with corresponding unstructured models (obtained by collapsing each annual matrix to a single survival and fertility rate) for three of our case study species: baneberry, scrub mint, and ground squirrels. Details of the case studies are provided in Table 2 and in sections 4.2, 4.3, and 4.4. We find that even though both the structured and unstructured models experience the same sequence of environmental variation, the model without population structure can produce inaccurate estimates of both population size and growth rate. This is because ignoring structure omits demographic memory and transient effects. The comparison highlights that variation in population growth rate is not driven by vital rates alone, but also by the stage structure on which those rates act.

## 4.1 Orcas

Orcas (*Orcinus orca*) are a long-lived marine mammal and a top predator in the ocean. We selected a series of projection matrices built from data on a population of "resident killer whales" in the Northeast Pacific Ocean (Vélez-Espino et al., 2014). There are 24 annual transition matrices, with the life cycle represented by a two-sex model with seven life stages: calves and juveniles (without sexes being separated), two stages of mature males (young and old), and three stages of females (young reproductive, old reproductive, and post-reproductive). The mean projection matrix yields a generation time of 32 years and an asymptotic population growth rate indicating slight declines in the long term ($\lambda_d = 0.989$).

In the orca population, the variation in vital rates is quite small, with coefficients of variation below 10% for all vital rates except calf survival, which has a CV of 13% (Figure 1A). As a result, the variance in population growth rate is very small ($\mathrm{Var}\lambda_t = 0.0013$). In contrast to our analytical expectation that long-lived species should have more contributions

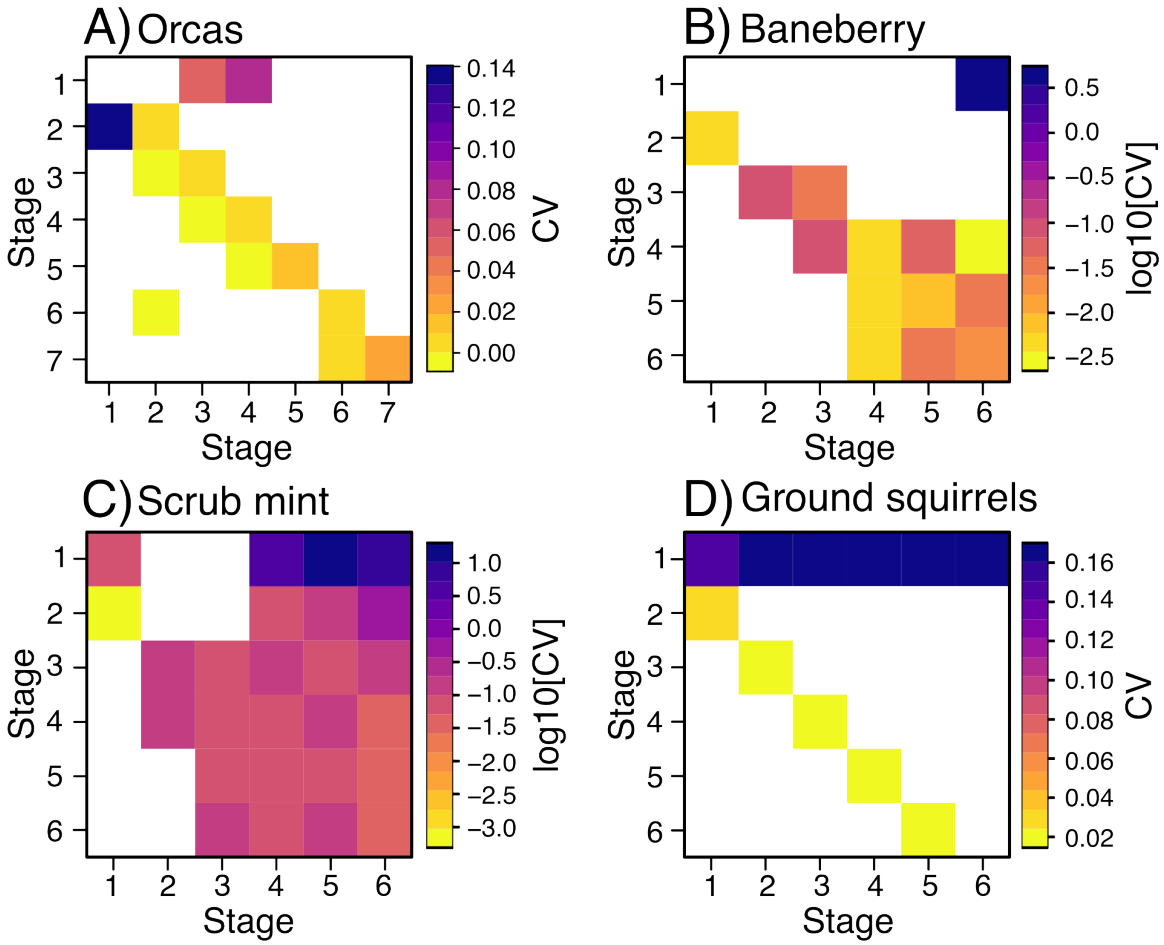


Figure 1: The four case studies show distinct patterns of variation in matrix elements. In each panel, the grid of boxes indicates the elements of the population projection matrix. The grid is colored according to the coefficient of variation for each matrix element across the time series of matrices. Note that the color scale is log-transformed for (B) baneberry and (C) scrub mint, but not for (A) orcas or (D) ground squirrels.

from variation in population structure, the small variation in population growth rate for these orcas is almost entirely due to variation in rates (Figure 2A). It is likely that the variation in vital rates was too small in this case to excite the population structure such that transient dynamics persist over multiple time steps.

### 4.2 Baneberry

Baneberry (*Actaea spicata*) is a perennial understory herb. We used a set of six projection matrices from a deciduous forest site in southeastern Sweden (Fröborg and Eriksson, 2003). The model represents the baneberry life cycle with six stages: seed, seedling, juvenile, small vegetative, large vegetative, and reproductive. This population has a generation time of 17 years, and the long-term population growth rate for the mean matrix is 0.975 (Table 2), indicating a declining population.

Most of the vital rates show a very small variation across years, with the exception of seed production, which has a CV of 342% (Figure 1B). The analytical and simulated results agree quite well, with vital rates and population structure each contributing approximately half of the variance in population growth rate (Figure 2B). Here, unlike with the orcas, the variation in vital rates (perhaps specifically variation in seed production) is large enough to generate perturbations to population structure that persist due to the long generation time.

### 4.3 Scrub mint

The endemic Florida scrub mint (*Dicerandra frutescens*) is an endangered herbaceous perennial found in fire-prone scrub environments. We selected a set of nine projection matrices collected in a sand pine scrub habitat site that was in a "long-unburned" state (Menges et al., 2006). The authors used matrix population models with six life stages: a persistent seedbank, seedlings, vegetative individuals and three sizes of flowering individuals (small, medium, and large). The mean projection matrix implies that the population had a generation time of 16 years and long-term population growth rate of 0.838 (Table 2).

The matrices for scrub mint (Figure 1C) exhibit high variation in the production of seeds (CV range 355 to 1048%), and moderate values of variation in production of seedlings (CV range 7 to 60%) and the matrix entries related to survival and transitions among the various adult stages (CV range 3 to 19%). As the result of this variation in vital rates, the variation in

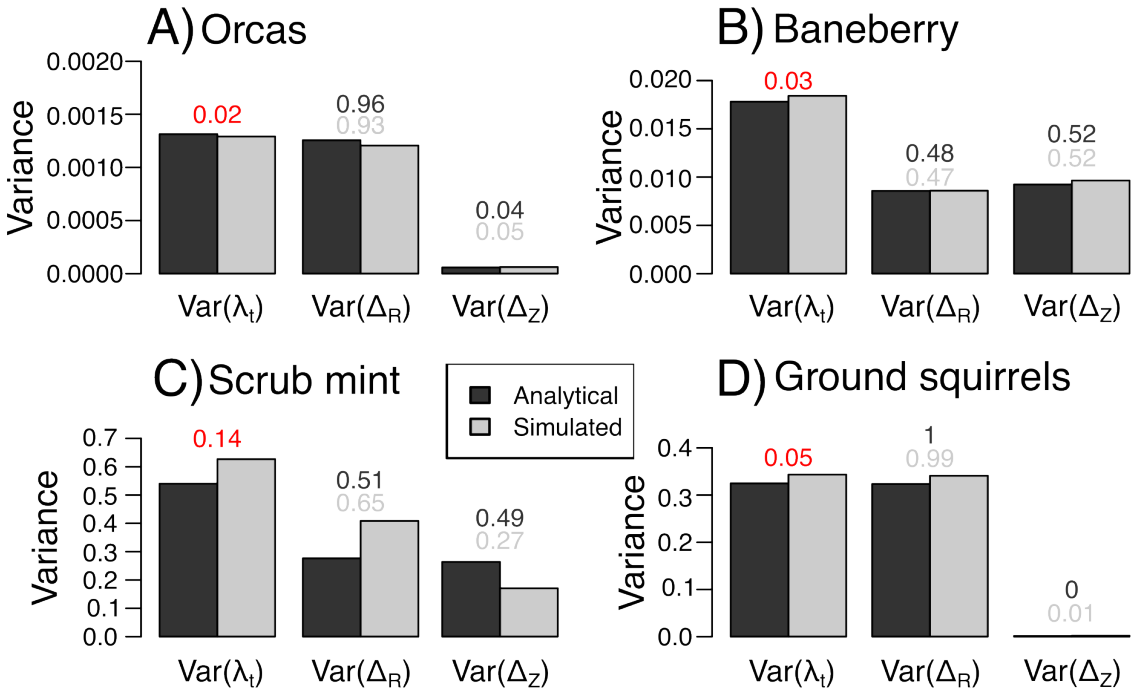


Figure 2: Decomposition of variance in population growth rate for the case studies. Each panel represents one case study, and shows the comparison between the analytical and simulation results for variance in $\lambda_t$, the contribution from variance in $\Delta_R$, and the contribution from variance in $\Delta_Z$. Note that y-axis limits differ among panels. Analytical terms are as given in Equations (10), (11), and their sum ($\text{Var}\lambda_t = \text{Var}(\Delta_R) + \text{Var}(\Delta_Z)$), while simulated terms are calculated directly from the simulations. The red number indicates the percent error between the analytical and simulated value of variance in $\lambda_t$ (treating the simulation as correct because the analytical result neglects interaction and covariance terms). The grey numbers above the $\text{Var}(\Delta_R)$ and $\text{Var}(\Delta_Z)$ bars indicate the proportion of $\text{Var}(\lambda_t)$ that is explained by each of the components.

population growth rate is markedly higher than for the orcas or baneberry cases. Furthermore, the analytical results do not match the simulation results that closely (14% error in overall variance in $\lambda_t$, Figure 2C). In the face of the very high variation in vital rates, the analytical results underestimate the contributions from vital rates, overestimate the contributions from population structure, and there is about an 8% contribution from interaction terms.

### 4.4 Ground squirrels

The golden-mantled ground squirrel (*Callospermophilus lateralis*) is a small striped ground squirrel that is widely distributed in western North America. We utilized a set of 18 projection matrices based on data collected at the Rocky Mountain Biological Laboratory in Colorado, USA (Hostetler et al., 2012). The age-based transition matrices have six classes, from young of the year to six years old (and no survival beyond age six). The generation time is one year, and long-term population growth rate is 2.05 (Table 2).

In this population, the vital rates and population growth rate show moderate interannual variation (Figure 1D). In particular, reproductive output has a CV of 16%, while survival parameters show much smaller variation with a CV of 2.4%. Still, this variation leads to fairly high variance in population growth rate (Figure 2D). However, it is worth remembering that variance tends to be correlated with the mean, and the long-term population growth rate for the squirrels is more than double the value for the other case studies (Table 2). We find that the variance in population growth rate is exclusively due to variation in vital rates, with no contributions from structure (Figure 2D). This matches our expectation due to their extremely short generation time, that transient dynamics (*i.e.*, fluctuations in population structure due to past variation in vital rates) decay quickly and therefore contribute little to variance in population growth rate.

## 5 Discussion

Population ecology fundamentally seeks to identify and understand the drivers of variation in population growth rate across time, space, and the Tree of Life (Sutherland et al., 2013). Variation across time is particularly important, because it can be generated by many processes, including environmental variability (Houston and McNamara, 1990; Vázquez et al.,

2017), biotic interactions (Levine et al., 2024), transient perturbations (Jaggi et al., 2026b; Wiedenmann et al., 2009), or interactions of these (*e.g.*, Coulson et al., 2001). Here, we focus on environmentally-driven variation in vital rates and the propensity of the population to "remember" past vital rate variation through transient fluctuations in population structure. We present a simple, robust framework for decomposing variation in population growth rate into contributions from variation in vital rates and contributions from variation in population structure. When we assume that the vital rates are drawn from a stationary distribution of possible environments, without auto-correlation, we can derive analytical results that predict when the contribution from vital rates or population structure should be greatest. The contribution of vital rate fluctuations to population growth rate will be highest when there is high variation in vital rates corresponding to dominant stages in the population structure. Meanwhile, variation in population structure will be greatest in populations with long generation time, where transient dynamics decay slowly. Our four case studies generally match these expectations, while also highlighting the importance of the magnitude of variation in vital rates.

We illustrate the importance of accounting for population structure by comparing structured and unstructured models. We find that ignoring population structure produces inaccurate and biased estimates of both population size and growth rate. Our decomposition is exact and differs from that in Ellis and Crone (2013). They decomposed the population growth rate in a given time step into what they call the asymptotic and transient components. However, their asymptotic component, as far as we can tell, is derived from the asymptotic properties of a projection matrix that appears at a particular time. Thus, their approach cannot capture changing vital rates that follow a stochastic process. In contrast to the earlier work, our mathematical decomposition of variance is derived directly for a stochastic population model and provides an exact and accurate decomposition. We present both analytical and simulation-based results, which generally agree well.

A promising approach for variance decomposition in temporally-variable structured population models is the transient Life Table Response Experiment (transient LTRE; Koons et al. 2016). Transient LTREs are a *retrospective* method, wherein a time series of past vital rates and population structure can be decomposed to understand contributions of specific vital rates, population structure, and their interactions (Cant et al., 2025; Koons et al., 2016). An

important extension of the transient LTRE approach further relates vital rates to environmental covariates (Knape et al., 2023). This extension enables the quantification of contributions from demographic stochasticity, defined as a mismatch between realized vital rates and those expected based on environmental covariates (Dobson et al., 2024). Past work using transient LTREs has found an important role for demographic stochasticity (23 or 56%) while population structure contributed less than 5% of variation in population growth rate (Dobson et al., 2024; Knape et al., 2023). Both of these studies are on small populations (10-120 individuals of a single sex) of relatively short-lived (generation time 2-5 years) species. These results are not surprising in light of the small population size and our analytical results that predict smaller contributions from population structure in short-lived species.

Our method is a valuable complement to transient LTRE analyses for decomposing variation in population growth rate. An important advantage of the transient LTRE method is that it does not require any assumptions about the distribution of environmental states. Meanwhile, our analytical results assume that the vital rates are drawn from a stationary distribution of environmental states, and our simulation results require long burn-in periods with a specified sampling distribution of environmental states. On the other hand, transient LTRE requires complete information on past states (*i.e.*, a time series of vital rates and population structure), while our method requires only temporally-replicated observations of vital rates. Furthermore, our method is better suited to explore hypotheses about the relative importance of transient dynamics under different environmental scenarios (*e.g.*, climate change, different disturbance return intervals, management strategies) or for different life history strategies.

One of the limitations in the analytical framework is that we assume the long-run expectation of perturbation to vital rates is 0 ($\mathcal{E}[\mathbf{H}_t]$). This means that environmental perturbations fluctuate around a stationary mean and that there is no directional trend such as warming (Johnson and Lyman, 2020) or increased drought frequency (Chiang et al., 2021), among others. Thus, the average projection matrix $\overline{\mathbf{A}}$ captures the mean demographic regime, and fluctuations are expressed through $\Delta_R$ and $\Delta_Z$. This is a common assumption in stochastic demography and holds for systems that exhibit interannual variability with no sustained trends (Tuljapurkar, 1990). The assumption also implies that the time-average of vital rate perturbations can be approximated by the expectation, which requires sufficiently long time-series (Tuljapurkar, 1990). Further research can examine what happens when vital rate pertur-

bations are temporally autocorrelated. Autocorrelated time series have 'memory' such that population sizes are negatively or positively correlated with past population sizes (Pilowsky and Dahlgren, 2020; Tuljapurkar and Haridas, 2006). Positive autocorrelation leads to sequences of "good" or "bad" years becoming longer whereas negative autocorrelation leads to alternating conditions, preventing long runs of favorable or unfavorable environments. In our framework, incorporating temporal autocorrelation does not change the decomposition for population growth rate in Eq. (4) but does change the variance equations. Recent studies (Francis et al., 2021; Morozov et al., 2024) have also highlighted the importance of 'long transients' that can last for hundreds of generations or even longer, and is another avenue for future research.

In examples where we find low variance in population growth rate ($\mathrm{Var}(\lambda_t) \approx 10^{-3}$ as in the orca case study), it is important to question whether that is a true signal or a result of parameter uncertainty. Recent research in demography has emphasized a lack of standardized protocol for uncertainty quantification, propagation, and reporting for matrix population models (Gascoigne et al., 2023; Simmonds and Jones, 2024). Indeed, these authors found that, while the reporting of demographic rate uncertainty is common for matrix population models, this reporting is inconsistent and often incomplete. Thus, when variance decomposition is applied to these models, errors in estimates of vital rates are propagated through estimates of $\lambda_t$. For instance, if estimation error in survival or reproduction rates is comparable to temporal fluctuations, then it may be challenging to tease apart the sources of variance in $\lambda_t$. In addition, estimating $\mathrm{Var}(\lambda_t)$ requires long-term demographic studies. However, available matrix population model studies are often too short to capture long-term fluctuations (Crone et al., 2013).

It is also important to note that our results do not focus on the magnitude of $\epsilon$, which corresponds to the size of perturbations. In the derivations, $\epsilon$ is a scaling parameter that allows us to separate the first and second order effects. However, in real ecological systems the size of perturbations can play an important role (Miller et al., 2012). Factors such as vital rate elasticities (Kajin et al., 2025), density-dependent trade-offs (Jaggi et al., 2024b), and demographic buffering (Gascoigne et al., 2025) determine how environmental variation translates into realized variability in survival, growth, and reproduction. Demographic mechanisms may dampen or amplify the effective magnitude of $\epsilon$.

Our framework provides an exact and conceptually transparent decomposition of temporal variation in population growth rate into contributions from vital-rate variability and transient population structure. By unifying stochastic demography with transient dynamics, this approach clarifies when demographic memory is expected to amplify or dampen environmental variability and how these effects depend on life-history strategy and covariance among rates. Unlike retrospective approaches (Knape et al., 2023; Koons et al., 2016), our method requires only temporally replicated demographic models and is therefore well suited for comparative analyses, cases where long time series of demographic data are not yet available, scenario testing, and forecasting under alternative environmental regimes. As long-term demographic datasets continue to accumulate and are increasingly used to inform management and conservation decisions, this approach offers a robust tool to disentangle extrinsic environmental forcing from intrinsic population responses, and to identify when transient dynamics are likely to play a dominant role in shaping population trajectories.

# References


Bienvenu, F., & Legendre, S. (2015). A new approach to the generation time in matrix population models. *American Naturalist*, *185*, 834–843. https://doi.org/10.1086/681104

Cant, J. I., Hernandez, C. M., Koons, D., Hodgson, D. J., Qi, M., Hector, A., Stott, I., & Salguero-Gomez, R. (2025). Life-history variation mediates the importance of population structure to the short-term dynamics of plant populations worldwide. *EcoEvoRxiv*. https://doi.org/10.32942/X2KD2S

Caswell, H. (1989). Analysis of life table response experiments: Decomposition of effects on population growth rate. *Ecological Modelling*, *46*, 221–237. https://doi.org/10.1016/0304-3800(89)90019-7

Caswell, H. (2001). *Matrix population models* (2nd ed.). Sinauer Associates.

Caswell, H. (2007). Sensitivity analysis of transient population dynamics. *Ecology letters*, *10*(1), 1–15.

Caswell, H. (2019). *Sensitivity analysis: Matrix methods in demography and ecology*. Springer Nature.

Chiang, F., Mazdiyasni, O., & AghaKouchak, A. (2021). Evidence of anthropogenic impacts on global drought frequency, duration, and intensity. *Nature communications*, *12*(1), 2754.

Coulson, T., Catchpole, E. A., Albon, S. D., Morgan, B. J. T., Pemberton, J. M., Clutton-Brock, T. H., Crawley, M. J., & Grenfell, B. T. (2001). Age, sex, density, winter weather, and population crashes in Soay sheep. *Science*, *292*(5521), 1528–1531. https://doi.org/10.1126/science.292.5521.1528

Crone, E. E., Ellis, M. M., Morris, W. F., Stanley, A., Bell, T., Bierzychudek, P., Ehrlen, J., Kaye, T. N., Knight, T. M., Lesica, P., et al. (2013). Ability of matrix models to explain the past and predict the future of plant populations. *Conservation Biology*, *27*(5), 968–978.

Crone, E. E., Menges, E. S., Ellis, M. M., Bell, T., Bierzychudek, P., Ehrlén, J., Kaye, T. N., Knight, T. M., Lesica, P., Morris, W. F., Oostermeijer, G., Quintana-Ascencio, P. F., Stanley, A., Ticktin, T., Valverde, T., & Williams, J. L. (2011). How do plant ecologists use matrix population models? *Ecology Letters*, *14*(1), 1–8. https://doi.org/10.1111/j.1461-0248.2010.01540.x

De Kroon, H., Van Groenendael, J., & Ehrlén, J. (2000). Elasticities: A review of methods and model limitations. *Ecology*, *81*(3), 607–618.

Dobson, F. S., Koons, D. N., Saraux, C., Tamian, A., Oli, M. K., & Viblanc, V. A. (2024). The demographic basis of population growth: A 32-year transient Life Table Response Experiment. *Ecology Letters*, *27*(12), e14512. https://doi.org/10.1111/ele.14512

Ellis, M. M., & Crone, E. E. (2013). The role of transient dynamics in stochastic population growth for nine perennial plants. *Ecology*, *94*(8), 1681–1686. https://doi.org/10.1890/13-0028.1

Ellner, S. P., Childs, D. Z., & Rees, M. (2016). *Data-driven modelling of structured populations: A practical guide to the integral projection model*. Springer International Publishing. https://doi.org/10.1007/978-3-319-28893-2_1

Francis, T. B., Abbott, K. C., Cuddington, K., Gellner, G., Hastings, A., Lai, Y.-C., Morozov, A., Petrovskii, S., & Zeeman, M. L. (2021). Management implications of long transients in ecological systems. *Nature Ecology & Evolution*, *5*(3), 285–294.

Fröborg, H., & Eriksson, O. (2003). Predispersal seed predation and population dynamics in the perennial understorey herb actaea spicata. *Canadian Journal of Botany*, *81*(11), 1058–1069. https://doi.org/10.1139/b03-099

Gascoigne, S. J., Kajin, M., Tuljapurkar, S., Santos, G. S., Compagnoni, A., Steiner, U. K., Vinton, A. C., Jaggi, H., Sepil, I., & Salguero-Gómez, R. (2025). Structured demographic buffering: A framework to explore the environmental components and demographic mechanisms underlying demographic buffering. *Ecology Letters*, *28*(2), e70066.

Gascoigne, S. J., Rolph, S., Sankey, D., Nidadavolu, N., Stell Pičman, A. S., Hernández, C. M., Philpott, M. E., Salam, A., Bernard, C., Fenollosa, E., et al. (2023). A standard protocol to report discrete stage-structured demographic information. *Methods in Ecology and Evolution*, *14*(8), 2065–2083.

Godoy, O., & Levine, J. M. (2014). Phenology effects on invasion success: Insights from coupling field experiments to coexistence theory. *Ecology*, *95*(3), 726–736.

Greenberg, D. A., & Green, D. M. (2013). Effects of an invasive plant on population dynamics in toads. *Conservation Biology*, *27*(5), 1049–1057. https://doi.org/https://doi.org/10.1111/cobi.12078

Haridas, C., & Tuljapurkar, S. (2005). Elasticities in variable environments: Properties and implications. *The American Naturalist*, *166*(4), 481–495.

Hastings, A. (2004). Transients: The key to long-term ecological understanding? *Trends in ecology & evolution*, *19*(1), 39–45.

Hastings, A., Abbott, K. C., Cuddington, K., Francis, T., Gellner, G., Lai, Y.-C., Morozov, A., Petrovskii, S., Scranton, K., & Zeeman, M. L. (2018). Transient phenomena in ecology. *Science*, *361*(6406), eaat6412.

Heppell, S. S., Caswell, H., & Crowder, L. B. (2000). Life histories and elasticity patterns: Perturbation analysis for species with minimal demographic data. *Ecology*, *81*(3), 654–665.

Hernández, C. M., Ellner, S. P., Adler, P. B., Hooker, G., & Snyder, R. E. (2023). An exact version of life table response experiment analysis, and the r package exactltre. *Methods in Ecology and Evolution*, *14*, 939–951. https://doi.org/10.1111/2041-210X.14065

Hone, J., Duncan, R. P., & Forsyth, D. M. (2010). Estimates of maximum annual population growth rates (rm) of mammals and their application in wildlife management. *Journal of Applied Ecology*, *47*(3), 507–514.

Hostetler, J. A., Kneip, E., Van Vuren, D. H., & Oli, M. K. (2012). Stochastic population dynamics of a montane ground-dwelling squirrel. *PloS one*, *7*(3), e34379.

Houston, A. I., & McNamara, J. M. (1990). The effect of environmental variability on growth. *Oikos*, 15–20.

Jaggi, H., Bassar, R., Travis, J., Nabeel, A., Reznick, D., & Levin, S. (2026a). Noise and determinism in trinidadian guppy population dynamics. *bioRxiv*, 2026–05.

Jaggi, H., Steinsaltz, D., & Tuljapurkar, S. (2024a). Temporal variability can promote migration between habitats. *Theoretical Population Biology*, *158*, 195–205.

Jaggi, H., Tuljapurkar, S., Zuo, W., Gascoigne, S. J., Kajin, M., & Salguero-Gómez, R. (2026b). Transient dynamics and nonlinear fitness: A matrix approach to pulse and press perturbation. *Ecology*, *107*(6), e70433.

Jaggi, H., Zuo, W., Kentie, R., Gaillard, J.-M., Coulson, T., & Tuljapurkar, S. (2024b). Density dependence shapes life-history trade-offs in a food-limited population. *Ecology Letters*, *27*(11), e14551.

Jiang, S., Jaggi, H., Zuo, W., Oli, M. K., Coulson, T., Gaillard, J.-M., & Tuljapurkar, S. (2022). Reproductive dispersion and damping time scale with life-history speed. *Ecology Letters*, *25*(9), 1999–2008.

Johnson, G. C., & Lyman, J. M. (2020). Warming trends increasingly dominate global ocean. *Nature Climate Change*, *10*(8), 757–761.

Kajin, M., Tuljapurkar, S., Zuo, W., Jaggi, H., Gascoigne, S., & Salguero-Gómez, R. (2025). Second-order elasticities for ecology and evolution: Unravelling nonlinear fitness responses to perturbations. *bioRxiv*, 2025–04.

Knape, J., Paquet, M., Arlt, D., Kačergytė, I., & Pärt, T. (2023). Partitioning variance in population growth for models with environmental and demographic stochasticity. *Journal of Animal Ecology*, *92*(10), 1979–1991. https://doi.org/10.1111/1365-2656.13990

Koons, D. N., Iles, D. T., Schaub, M., & Caswell, H. (2016). A life-history perspective on the demographic drivers of structured population dynamics in changing environments. *Ecology Letters*, *19*(9), 1023–1031. https://doi.org/10.1111/ele.12628

Koons, D. N., Rockwell, R. F., & Grand, J. B. (2006). Population Momentum: Implications for Wildlife Management. *Journal of Wildlife Management*, *70*(1), 19–26. https://doi.org/10.2193/0022-541X(2006)70[19:PMIFWM]2.0.CO;2

Levine, J. M., HilleRisLambers, J., Petry, W. K., Usinowicz, J., & Crowther, T. W. (2024). Demographic but not competitive time lags can transiently amplify climate-induced changes in vegetation carbon storage. *Global Change Biology*, *30*(8), e17432.

Lindell, T., Ehrlén, J., & Dahlgren, J. P. (2022). Weather-driven demography and population dynamics of an endemic perennial plant during a 34-year period. *Journal of Ecology*, *110*(3), 582–592. https://doi.org/https://doi.org/10.1111/1365-2745.13821

Maldonado-Chaparro, A. A., Blumstein, D. T., Armitage, K. B., & Childs, D. Z. (2018). Transient LTRE analysis reveals the demographic and trait-mediated processes that buffer population growth. *Ecology Letters*, *21*(11), 1693–1703. https://doi.org/10.1111/ele.13148

McDonald, J. L., Stott, I., Townley, S., & Hodgson, D. J. (2016). Transients drive the demographic dynamics of plant populations in variable environments. *Journal of Ecology*, *104*(2), 306–314. https://doi.org/10.1111/1365-2745.12528

Menges, E. S., Ascencio, P. F. Q., Weekley, C. W., & Gaoue, O. G. (2006). Population viability analysis and fire return intervals for an endemic florida scrub mint. *Biological conservation*, *127*(1), 115–127.

Metz, J. A. J., Nisbet, R. M., & Geritz, S. A. H. (1992). How should we define 'fitness' for general ecological scenarios? *Trends in Ecology and Evolution*, *7*(6), 198–202.

Miller, A., Reilly, D., Bauman, S., & Shea, K. (2012). Interactions between frequency and size of disturbance affect competitive outcomes. *Ecological research*, *27*(4), 783–791.

Morozov, A., Feudel, U., Hastings, A., Abbott, K. C., Cuddington, K., Heggerud, C. M., & Petrovskii, S. (2024). Long-living transients in ecological models: Recent progress, new challenges, and open questions. *Physics of Life Reviews*, *51*, 423–441.

Oldfather, M. F., & Ackerly, D. D. (2019). Microclimate and demography interact to shape stable population dynamics across the range of an alpine plant. *New Phytologist*, *222*(1), 193–205. https://doi.org/https://doi.org/10.1111/nph.15565

Paniw, M., James, T. D., Ruth Archer, C., Römer, G., Levin, S., Compagnoni, A., Che-Castaldo, J., Bennett, J. M., Mooney, A., Childs, D. Z., Ozgul, A., Jones, O. R.,

Burns, J. H., Beckerman, A. P., Patwary, A., Sanchez-Gassen, N., Knight, T. M., & Salguero-Gómez, R. (2021). The myriad of complex demographic responses of terrestrial mammals to climate change and gaps of knowledge: A global analysis. *Journal of Animal Ecology*, *90*(6), 1398–1407. https://doi.org/10.1111/1365-2656.13467

Pilowsky, J. A., & Dahlgren, J. P. (2020). Incorporating the temporal autocorrelation of demographic rates into structured population models. *Oikos*, *129*(2), 238–248.

Robey, A. J., Kummel, M. T., & Vasseur, D. A. (2025). Temporal autocorrelation increases temperature-driven extinction risk by clustering stressful conditions. *bioRxiv*, 2025–07.

Rudgers, J. A., & Hoeksema, J. D. (2003). Inter-annual variation in above-and belowground herbivory on a native, annual legume. *Plant Ecology*, *169*(1), 105–120. https://doi.org/10.1023/A:1026221602968

Salguero-Gómez, R., Jones, O. R., Archer, C. R., Bein, C., de Buhr, H., Farack, C., Gottschalk, F., Hartmann, A., Henning, A., Hoppe, G., Römer, G., Ruoff, T., Sommer, V., Wille, J., Voigt, J., Zeh, S., Vieregg, D., Buckley, Y. M., Che-Castaldo, J., ... Vaupel, J. W. (2016). COMADRE: A global data base of animal demography. *Journal of Animal Ecology*, *85*(2), 371–384. https://doi.org/10.1111/1365-2656.12482

Salguero-Gómez, R., Jones, O. R., Archer, C. R., Buckley, Y. M., Che-Castaldo, J., Caswell, H., Hodgson, D., Scheuerlein, A., Conde, D. A., Brinks, E., Buhr, H., Farack, C., Gottschalk, F., Hartmann, A., Henning, A., Hoppe, G., Römer, G., Runge, J., Ruoff, T., ... Vaupel, J. W. (2015). The COMPADRE plant matrix database: An open online repository for plant demography. *Journal of Ecology*, *103*, 202–218. https://doi.org/10.1111/1365-2745.12334

Sibly, R. M., & Hone, J. (2002). Population growth rate and its determinants: An overview. *Philosophical Transactions of the Royal Society of London. Series B: Biological Sciences*, *357*(1425), 1153–1170.

Simmonds, E. G., & Jones, O. R. (2024). Uncertainty propagation in matrix population models: Gaps, importance and guidelines. *Methods in Ecology and Evolution*, *15*(2), 427–438.

Stott, I., Townley, S., Carslake, D., & Hodgson, D. J. (2010). On reducibility and ergodicity of population projection matrix models. *Methods in Ecology and Evolution*, *1*(3), 242–252. https://doi.org/10.1111/j.2041-210X.2010.00032.x

Stott, I., Townley, S., & Hodgson, D. J. (2011). A framework for studying transient dynamics of population projection matrix models. *Ecology Letters*, *14*(9), 959–970. https://doi.org/10.1111/j.1461-0248.2011.01659.x

Summers, J., Cosgrove, E. J., Bowman, R., Fitzpatrick, J. W., & Chen, N. (2024). Density dependence maintains long-term stability despite increased isolation and inbreeding in the Florida Scrub-Jay. *Ecology Letters*, *27*(12), e14483. https://doi.org/10.1111/ele.14483

Sutherland, W. J., Freckleton, R. P., Godfray, H. C. J., Beissinger, S. R., Benton, T., Cameron, D. D., Carmel, Y., Coomes, D. A., Coulson, T., Emmerson, M. C., et al. (2013). Identification of 100 fundamental ecological questions. *Journal of Ecology*, *101*(1), 58–67.

Sutherland, W. J., & Norris, K. (2002). Behavioural models of population growth rates: Implications for conservation and prediction. *Philosophical Transactions of the Royal Society of London. Series B: Biological Sciences*, *357*(1425), 1273–1284.

Thomas, M. B. (1999). Ecological approaches and the development of "truly integrated" pest management. *Proceedings of the National Academy of Sciences*, *96*(11), 5944–5951.

Tuljapurkar, S. (1990). *Population dynamics in variable environments*. Springer.

Tuljapurkar, S., & Haridas, C. (2006). Temporal autocorrelation and stochastic population growth. *Ecology letters*, *9*(3), 327–337.

Tuljapurkar, S., Horvitz, C. C., & Pascarella, J. B. (2003). The many growth rates and elasticities of populations in random environments. *The American Naturalist*, *162*(4), 489–502.

Vázquez, D. P., Gianoli, E., Morris, W. F., & Bozinovic, F. (2017). Ecological and evolutionary impacts of changing climatic variability. *Biological Reviews*, *92*(1), 22–42.

Vélez-Espino, L. A., Ford, J. K. B., Araujo, H., Ellis, G., Parken, C., & Balcomb, K. (2014). *Comparative demography and viability of northeastern pacific resident killer whale populations at risk*. Fisheries; Oceans Canada= Pêches et océans Canada.

Wiedenmann, J., Fujiwara, M., & Mangel, M. (2009). Transient population dynamics and viable stage or age distributions for effective conservation and recovery. *Biological Conservation*, *142*(12), 2990–2996.

# Appendices for "A robust method for quantifying the contribution of transient dynamics to variation in population growth rate"



## S1 Contribution of population structure to population growth rate

To illustrate the importance of population structure, we compare projections from structured matrix population models with those from unstructured models obtained by collapsing each matrix to a single survival and fertility rate. Although both models experience the same sequence of environmental variation, the rates differ between unstructured and structured population growth rates as well as realized population sizes. One of the reasons is that the unstructured model assumes that the population is close to stable stage distribution, thereby ignoring the contribution of population structure. As shown in Figure S1, this simplification can lead to substantial discrepancies in both realized growth rates and population size trajectories. We want to note that this collapse is not well-defined for the orca model because the

matrices exhibit near-stasis in some stages (i.e., transition probabilities equal to one) which makes the comparison unreliable. Hence we excluded orcas for comparison between structured and unstructured population size and growth rate.

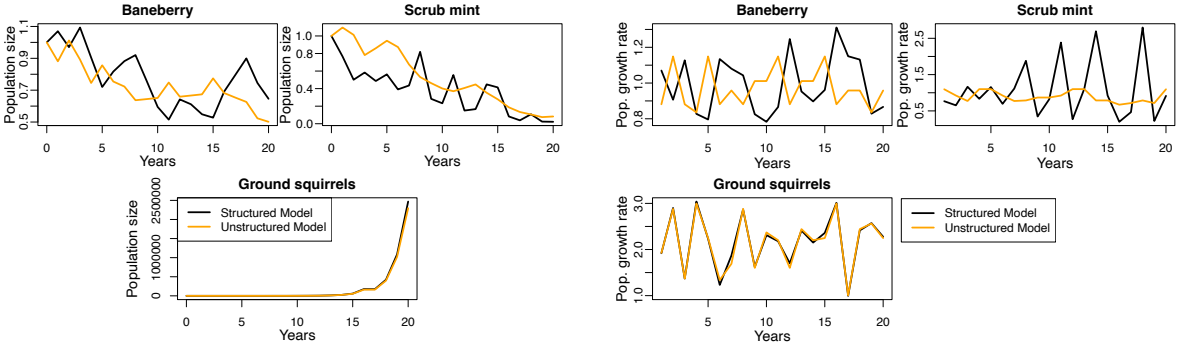


(a) Comparison of population size trajectories.

(b) Comparison of population growth rates.

Figure S1: Comparison between structured and unstructured models. The left panels compare population size trajectories and the right panels compare realized population growth rates between unstructured model (yellow) and structured model (black). We compare these across three species: baneberry, scrub mint, and ground squirrel in both the panels.

## S2 Decomposition of the average matrix

Let the dominant eigenvalue of the average projection matrix, $\overline{\mathbf{A}}$ be $\lambda_d$. Let $\mathbf{u}$ and $\mathbf{v}$ be the corresponding right and left eigenvectors, respectively. The vector $\mathbf{u}$ is the stable population structure and $\mathbf{v}$ is the reproductive value. Normalize $\mathbf{u}$ and $\mathbf{v}$ so that $(\mathbf{e}, \mathbf{u}) = 1$ and $(\mathbf{v}, \mathbf{u}) = 1$. Thus we have:

$$\overline{\mathbf{A}}\mathbf{u} = \lambda_d \mathbf{u} \iff \lambda_d = (\mathbf{e}, \overline{\mathbf{A}}\mathbf{u}) \iff \mathbf{u} = \frac{\overline{\mathbf{A}}\mathbf{u}}{(\mathbf{e}, \overline{\mathbf{A}}\mathbf{u})}. \tag{S1}$$

Next, we introduce the projection operator

$$\mathbf{P} = \mathbf{u}\,\mathbf{v}^T = \mathbf{P}^2. \tag{S2}$$

The matrix $\mathbf{P}$ projects the system in the asymptotic direction defined by the dominant eigenvectors $\mathbf{u}$ and $\mathbf{v}$ (Jaggi et al., 2026). By the Perron-Frobenius theorem (Caswell, 2012), we can decompose the mean projection matrix ($\overline{\mathbf{A}}$) into two components:

$$\overline{\mathbf{A}} = \lambda_d(\mathbf{P} + \mathbf{Q}) \tag{S3}$$

where $\mathbf{P}$ captures the asymptotic dynamics and $\mathbf{Q}$ governs the transient deviations (Jaggi et al., 2026). Note that $\mathbf{P}$ and $\mathbf{Q}$ are orthogonal, that is, $\mathbf{PQ} = 0$. Normalizing by $\lambda_d$:

$$\mathbf{B} = \frac{\overline{\mathbf{A}}}{\lambda_d} = (\mathbf{P} + \mathbf{Q}), \tag{S4}$$

$$\mathbf{B}^m = \mathbf{P} + \mathbf{Q}^m, \text{ for } m \geq 1, \tag{S5}$$

the effect of $\mathbf{Q}$ decays over time as:

$$\mathbf{Q}^m \to 0 \propto \rho^m, \text{ with } 0 < \rho < 1, \tag{S6}$$

where $\rho$ is the asymptotic damping rate and determines the rate at which populations converge to a stable stage distribution. Thus, $\mathbf{P}$ represents the projection of the system along $\lambda_d$ and is associated with the asymptotic dynamics whereas $\mathbf{Q}$ (orthogonal to $\mathbf{P}$) is the part associated with transient dynamics. Across comparative datasets, Jiang et al. (2022) showed that damping time $\tau = -\frac{1}{\log \rho}$ increased with generation time as:

$$\tau \propto T_c \text{ where } T_c \text{ is the cohort generation time.}$$

Therefore, we can expect that species with a long generation time will exhibit slower decay of transient dynamics.

## S3 Small-noise approximation

In the main manuscript, we define the observed deviations $\mathbf{H}_t = \mathbf{A}_t - \overline{\mathbf{A}}$ and $\mathbf{z}_t = \mathbf{w}_t - \overline{\mathbf{w}}$. Adopting an assumption of small fluctuations ("small noise"), the first order approximations can be written as:

$$\mathbf{A}_t = \overline{\mathbf{A}} + \epsilon \mathbf{H}_t \text{ and } \mathbf{w}_t = \overline{\mathbf{w}} + \epsilon \mathbf{z}_t \tag{S7}$$

where $\mathcal{E}[\mathbf{H}_t] = 0$ and $(\mathbf{e}, \mathbf{z}_t) = 0$. Note that setting $\epsilon = 1$ recovers the notation and exact empirical decomposition in the main manuscript.

We define

$$\mathbf{G}_t = \frac{\mathbf{H}_t}{\lambda_d} \text{ and } \eta_t = \frac{\lambda_t}{\lambda_d} \tag{S8}$$

Using $\mathbf{B} = \overline{\mathbf{A}}/\lambda_d$ from Equation (S4) and substituting (S8), we get

$$\frac{\mathbf{A}_t}{\lambda_d} = \mathbf{B} + \epsilon \mathbf{G}_t, \text{ where } \mathcal{E}[\mathbf{G}_t] = 0. \tag{S9}$$

We can rewrite the age-structure iteration in (S7) as

$$\mathbf{w}_t = \frac{(\mathbf{B} + \epsilon \mathbf{G}_t)\, \mathbf{w}_{t-1}}{\eta_t}, \text{ where } \quad \eta_t = \frac{\lambda_t}{\lambda_d} = (\mathbf{e}, (\mathbf{B} + \epsilon \mathbf{G}_t)\mathbf{w}_{t-1}) \tag{S10}$$

Under stationary and zero-mean fluctuations, $\overline{\mathbf{w}} = \mathbf{u} + \mathcal{O}(\epsilon^2)$. Considering the numerator in (S10) and keeping terms to order $\epsilon$, we get,

$$\begin{aligned}
(\mathbf{B} + \epsilon \mathbf{G}_t)\, \mathbf{w}_{t-1} =& (\mathbf{B} + \epsilon \mathbf{G}_t)\, (\overline{\mathbf{w}} + \epsilon \mathbf{z}_{t-1}) && \text{(S11)} \\
=& \mathbf{B}\overline{\mathbf{w}} + \epsilon \mathbf{B}\mathbf{z}_{t-1} + \epsilon \mathbf{G}_t \overline{\mathbf{w}} + O(\epsilon^2) && \text{(S12)} \\
\approx& \mathbf{B}\mathbf{u} + \epsilon \mathbf{B}\mathbf{z}_{t-1} + \epsilon \mathbf{G}_t \overline{\mathbf{w}} && \text{(S13)} \\
=& \mathbf{u} + \epsilon \mathbf{B}\mathbf{z}_{t-1} + \epsilon \mathbf{G}_t \overline{\mathbf{w}} && \text{(S14)}
\end{aligned}$$

Similarly, the demoninator $\eta_t$ can be written to first order as:

$$\begin{aligned}
\eta_t =& (\mathbf{e}, \mathbf{B}\overline{\mathbf{w}}) + \epsilon\, (\mathbf{e}, \mathbf{B}\mathbf{z}_{t-1}) + \epsilon\, (\mathbf{e}, \mathbf{G}_t \overline{\mathbf{w}}) && \text{(S15)} \\
=& (\mathbf{e}, \mathbf{B}\mathbf{u}) + \epsilon\, (\mathbf{e}, \mathbf{B}\mathbf{z}_{t-1}) + \epsilon\, (\mathbf{e}, \mathbf{G}_t \overline{\mathbf{w}}) && \text{(S16)} \\
=& (\mathbf{e}, \mathbf{u}) + \epsilon\, (\mathbf{e}, \mathbf{B}\mathbf{z}_{t-1}) + \epsilon\, (\mathbf{e}, \mathbf{G}_t \overline{\mathbf{w}}) && \text{(S17)} \\
=& 1 + \epsilon\, (\mathbf{e}, \mathbf{B}\mathbf{z}_{t-1}) + \epsilon\, (\mathbf{e}, \mathbf{G}_t \overline{\mathbf{w}}) && \text{(S18)} \\
=& 1 + \epsilon \alpha_t && \text{(S19)}
\end{aligned}$$

where $\alpha_t = (\mathbf{e}, (\mathbf{B}\mathbf{z}_{t-1} + \mathbf{G}_t \overline{\mathbf{w}}))$ is a scalar.

The above expressions give us the numerator and denominator for equation (S10):

$$\mathbf{w}_t = \frac{(\mathbf{B} + \epsilon \mathbf{G}_t)\, \mathbf{w}_{t-1}}{\eta_t} \tag{S20}$$

$$= (\mathbf{u} + \epsilon \mathbf{B}\mathbf{z}_{t-1} + \epsilon \mathbf{G}_t \overline{\mathbf{w}})\, \eta_t^{-1} \tag{S21}$$

$$= (\mathbf{u} + \epsilon \mathbf{B}\mathbf{z}_{t-1} + \epsilon \mathbf{G}_t \overline{\mathbf{w}})\, (1 + \epsilon \alpha_t)^{-1}, \text{ take binomial approximation} \tag{S22}$$

$$= (\mathbf{u} + \epsilon \mathbf{B}\mathbf{z}_{t-1} + \epsilon \mathbf{G}_t \overline{\mathbf{w}})\, (1 - \epsilon \alpha_t), \text{ expand to first order} \tag{S23}$$

$$\approx \mathbf{u} + \epsilon \mathbf{B}\mathbf{z}_{t-1} + \epsilon \mathbf{G}_t \overline{\mathbf{w}} - \epsilon \alpha_t \mathbf{u} \tag{S24}$$

$$\mathbf{w}_t = \mathbf{u} + \epsilon \left(\mathbf{B}\mathbf{z}_{t-1} + \mathbf{G}_t \overline{\mathbf{w}} - \alpha_t \mathbf{u}\right) \tag{S25}$$

But we know $\mathbf{w}_t = \overline{\mathbf{w}} + \epsilon \mathbf{z}_t = \mathbf{u} + \epsilon \mathbf{z}_t$. Comparing this with equation (S25), we get the dynamics of deviations in population structure ($\mathbf{z}_t$) as:

$$\mathbf{z}_t = \mathbf{B}\mathbf{z}_{t-1} + \mathbf{G}_t \overline{\mathbf{w}} - \alpha_t \mathbf{u} \tag{S26}$$

$$= \mathbf{B}\mathbf{z}_{t-1} + \mathbf{G}_t \overline{\mathbf{w}} - (\mathbf{e}, (\mathbf{B}\mathbf{z}_{t-1} + \mathbf{G}_t \overline{\mathbf{w}}))\, \mathbf{u} \tag{S27}$$

$$= \mathbf{B}\mathbf{z}_{t-1} + \mathbf{G}_t \overline{\mathbf{w}} - \mathbf{e}^T (\mathbf{B}\mathbf{z}_{t-1} + \mathbf{G}_t \overline{\mathbf{w}}) \mathbf{u} \tag{S28}$$

$$= \left(\mathbf{I} - \mathbf{e}^T \mathbf{u}\right) (\mathbf{B}\mathbf{z}_{t-1} + \mathbf{G}_t \overline{\mathbf{w}}) \tag{S29}$$

$$\boxed{\mathbf{z}_t = \mathbf{K} (\mathbf{B}\mathbf{z}_{t-1} + \mathbf{G}_t \overline{\mathbf{w}})} \tag{S30}$$

where $\mathbf{K} = 1 - \mathbf{u}\, \mathbf{e}^T$. We also know that $\lambda_t = \lambda_d \eta_t$. Substituting the equation for $\eta_t$ in (S19), we get

$$\lambda_t = \lambda_d \left(1 + \epsilon \left(\mathbf{e}, \mathbf{B}\mathbf{z}_{t-1}\right) + \epsilon \left(\mathbf{e}, \mathbf{G}_t \overline{\mathbf{w}}\right)\right) \tag{S31}$$

$$\boxed{\lambda_t = \lambda_d + \epsilon \Delta_Z + \epsilon \Delta_R} \tag{S32}$$

where $\Delta_Z = \lambda_d \left(\mathbf{e}, \mathbf{B}\mathbf{z}_{t-1}\right)$ results from fluctuations in population structure and $\Delta_R = \lambda_d \left(\mathbf{e}, \mathbf{G}_t \mathbf{u}\right)$ captures fluctuations in demographic rates. Thus, we decompose $\lambda_t$ into the deterministic component $\lambda_d$ and two first-order contributions from fluctuation in population structure ($\Delta_Z$) and from fluctuation in demographic rates ($\Delta_R$).

Thus, we have a decomposition for the population growth rate as:

$$\lambda_t = \left(\mathbf{e}, (\overline{\mathbf{A}} + \epsilon\mathbf{H}_t)(\overline{\mathbf{w}} + \epsilon\mathbf{z}_{t-1})\right) \tag{S33}$$

$$\lambda_t = \lambda_0 + \epsilon\Delta_Z + \epsilon\Delta_R \tag{S34}$$

where

$$\lambda_0 = (\mathbf{e}, \overline{\mathbf{A}}\overline{\mathbf{w}}) \tag{S35}$$

$$\Delta_Z = (\mathbf{e}, \overline{\mathbf{A}}\mathbf{z}_{t-1}) \tag{S36}$$

$$\Delta_R = (\mathbf{e}, \mathbf{H}_t\overline{\mathbf{w}}) \tag{S37}$$

Equation (S34) becomes the exact decomposition in equation (4) of the main text when $\epsilon = 1$. To first order, $\overline{\mathbf{w}}$ can be replaced by $\mathbf{u}$ and $\lambda_0$ by $\lambda_d$, giving

$$\lambda_t = \lambda_d + \epsilon\lambda_d\left[(\mathbf{e}, \mathbf{B}\mathbf{z}_{t-1}) + (\mathbf{e}, \mathbf{G}_t\mathbf{u})\right] \tag{S38}$$

## S4 Expectation for $\lambda_t$

Taking expectations in equation (S38), we get

$$\mathcal{E}[\lambda_t] = \lambda_d + \epsilon\mathcal{E}[\Delta_Z] + \epsilon\mathcal{E}[\Delta_R] \tag{S39}$$

Because $\overline{\mathbf{w}}$ is the long-run mean population structure, $\mathcal{E}[\mathbf{z}_t] = 0$ by definition; because $\overline{\mathbf{A}}$ is the mean projection matrix, $\mathcal{E}[\mathbf{H}_t] = 0$. Consequently,

$$\mathcal{E}[\Delta_Z] = 0, \qquad \mathcal{E}[\Delta_R] = 0 \tag{S40}$$

The interaction term $\mathcal{E}[\Delta_{ZR}]$ need not be zero in general. It is zero when the current perturbation $\mathbf{H}_t$ is independent of the previous population structure $\mathbf{z}_{t-1}$, as under the independent and identically distributed environmental sequence assumed for the analytical results. Under this assumption:

$$\mathcal{E}[\lambda_t] = \lambda_0 = \lambda_d \tag{S41}$$

and therefore $\mathcal{E}[\lambda_t] = \lambda_d$ to first order. In these expressions, we do not consider the higher-order interaction terms. However, with temporal environmental autocorrelation or density-dependent feedback, $\mathbf{H}_t$ and $\mathbf{z}_{t-1}$ can be correlated and in this case, the interaction term $\mathcal{E}[\Delta_{ZR}]$ will remain.

## S5 Variance for $\lambda_t$

We now apply the variance formula $\mathrm{Var}(\lambda_t) = \mathcal{E}[(\lambda_t - \mathcal{E}(\lambda_t))^2]$ around the expectation $\mathcal{E}[\lambda_t] = \lambda_d + \epsilon\mathcal{E}[\Delta_Z] + \epsilon\mathcal{E}[\Delta_R] + \epsilon^2\mathcal{E}[\Delta_{ZR}]$, to obtain the variance decomposition as follows:

$$\begin{aligned}\mathrm{Var}(\lambda_t) = {} & \epsilon^2\mathrm{Var}(\Delta_Z) + \epsilon^2\mathrm{Var}(\Delta_R) + 2\epsilon^2\mathrm{Cov}(\Delta_Z, \Delta_R) \\ & + 2\epsilon^3\mathrm{Cov}(\Delta_Z, \Delta_{ZR}) + 2\epsilon^3\mathrm{Cov}(\Delta_R, \Delta_{ZR}) + \epsilon^4\mathrm{Var}(\Delta_{ZR}). \end{aligned} \tag{S42}$$

This is equation (9) in the main text. We make additional assumptions for a simpler expression as discussed in the main manuscript. We assume: (i) the fluctuations are small, and (ii) $\mathbf{H}_t$ is independent and identically distributed through time. Then $\mathbf{H}_t$ is independent of past fluctuations $\mathbf{z}_t$. As a result, we can drop the covariance term $\mathrm{Cov}(\Delta_Z, \Delta_R)$ and the interaction terms on the order of $\epsilon^3$ or higher.

Thus, from the previous expressions we approximate the variance in growth rate as:

$$\boxed{\mathrm{Var}(\lambda_t) \approx \mathrm{Var}(\Delta_Z) + \mathrm{Var}(\Delta_R)} \tag{S43}$$

Here,

- The first term represents the variance due to fluctuations in the population structure. These fluctuations capture the accumulated effects of past variation in vital rates.
- The second term represents the variance due to random perturbations in the vital rates (*i.e.* in elements of the population projection matrix) at time $t$. We have assumed that our population reaches stationarity, meaning that the perturbations are drawn from a distribution that does not depend on $t$. This implies that the magnitude of variance is the same for every $t$.

- Note that there may also be a covariance term between $\Delta_Z$ and $\Delta_R$. When the perturbations are iid (*i.e.,* independent and identically distributed, drawn from the stationary distribution of perturbations), then $\mathbf{G}_t$ is independent of $\mathbf{z}_{t-1}$ and therefore the covariance term is 0. Otherwise, it may be nonzero.

Thus, the variance in the growth rate $\lambda_t$ is influenced primarily by the variances in $\Delta_Z$ and $\Delta_R$, and their covariance. Next we will further derive for terms in the expression for $\mathrm{Var}(\lambda_t)$ as shown below.

#### S5.0.1 Derivation of $\mathbf{Var}(\Delta_R)$

We know that $\Delta_R = \lambda_d(\mathbf{e}, \mathbf{G}_t\mathbf{u})$ and so

$$\mathrm{Var}[\Delta_R] = \mathcal{E}\left[(\lambda_d \mathbf{e}^T \mathbf{G}_t \mathbf{u})^2\right] \tag{S44}$$

$$= \mathcal{E}\left[(\mathbf{e}^T \mathbf{H}_t \mathbf{u})^2\right], \tag{S45}$$

$$= \mathcal{E}\left[\left(\mathbf{e}^T \otimes \mathbf{e}^T\right)\left(\mathbf{H}_1 \otimes \mathbf{H}_1\right)\left(\mathbf{u} \otimes \mathbf{u}\right)\right], \tag{S46}$$

$$= \left(\mathbf{e}^T \otimes \mathbf{e}^T\right) \mathcal{E}\left[\mathbf{H}_1 \otimes \mathbf{H}_1\right]\left(\mathbf{u} \otimes \mathbf{u}\right), \tag{S47}$$

$$\boxed{\mathrm{Var}[\Delta_R] = \left(\mathbf{e}^T \otimes \mathbf{e}^T\right) \Sigma_1 \left(\mathbf{u} \otimes \mathbf{u}\right)} \tag{S48}$$

where $\Sigma_1 = \mathcal{E}\left[\mathbf{H}_1 \otimes \mathbf{H}_1\right]$. In step two of this derivation, we used $\lambda_d \mathbf{G}_t = \mathbf{H}_t$. In step 3, we used the Kronecker product and set $t = 1$; we could have used any $t$ due to stationarity. In step 4, we moved the expectation to the random bit. In steps 5 we identified that the expectation of the Kronecker product of random fluctuations is the var-cov matrix $\Sigma_1$ of the fluctuations in the matrix elements.

The equation (S48) therefore shows the immediate contribution of vital-rate variation depends on both the magnitude and the covariance structure of the perturbations and on the weighting by the stable stage distribution.

The analytical insight here is that the variation in $\lambda_t$ that is contributed by the fluctuations in vital rates is equivalent to the sum of the variance in vital rates weighted by the stable population distribution. The analytical predictions here are:

(1) the effect of varying rates depends on the size of fluctuations, as well as the representation of those sizes in the stable structure.

(2) overall variance in growth rates can be held down by negative correlations between rates.

(3) this component of variance in growth rate does not depend on serial correlation.

### S5.0.2 Derivation of Var($\Delta_Z$)

The variance of $\Delta_Z = \lambda_d(\mathbf{e}, \mathbf{B}\mathbf{z}_{t-1})$ is:

$$\mathrm{Var}(\Delta_Z) = \lambda_d^2 \mathcal{E}[(\mathbf{e}^T \mathbf{B}\mathbf{z}_{t-1})^2].$$

The last term above is

$$\mathcal{E}\left[(\mathbf{e}^T \mathbf{B}\mathbf{z}_{t-1})^2\right] = \mathcal{E}\left[\left(\mathbf{e}^T \otimes \mathbf{e}^T\right)\left(\mathbf{B}\mathbf{z}_{t-1} \otimes \mathbf{B}\mathbf{z}_{t-1}\right)\right]. \tag{S49}$$

We now return to Equation (S30) which we write again here for convenience:

$$\mathbf{z}_t = \mathbf{K}\left(\mathbf{B}\mathbf{z}_{t-1} + \mathbf{G}_t\mathbf{u}\right), \quad \mathbf{K} = 1 - \mathbf{u}\,\mathbf{e}^T.$$

Take Kronecker products and expectations to get:

$$\mathcal{E}\left[\mathbf{z}_t \otimes \mathbf{z}_t\right] = \left[\mathbf{K}\mathbf{B} \otimes \mathbf{K}\mathbf{B}\right] \mathcal{E}\left[\mathbf{z}_{t-1} \otimes \mathbf{z}_{t-1}\right] + \left[\mathbf{K} \otimes \mathbf{K}\right]\left[\mathbf{G}_t \otimes \mathbf{G}_t\right]\left[\mathbf{u} \otimes \mathbf{u}\right]. \tag{S50}$$

Stationarity means that the var-cov of $\mathbf{z}_t$ (*i.e.*, the Kronecker product of $\mathbf{z}_t$ with itself) at $t$ and $t-1$ are the same, so we can now solve to get:

$$\mathcal{E}\left[\mathbf{z}_t \otimes \mathbf{z}_t\right] = \left[\mathbf{K}\mathbf{B} \otimes \mathbf{K}\mathbf{B}\right] \mathcal{E}\left[\mathbf{z}_t \otimes \mathbf{z}_t\right] + \left[\mathbf{K} \otimes \mathbf{K}\right]\left[\mathbf{G}_t \otimes \mathbf{G}_t\right]\left[\mathbf{u} \otimes \mathbf{u}\right] \tag{S51}$$

$$\mathcal{E}\left[\mathbf{z}_t \otimes \mathbf{z}_t\right] = \left(\mathbf{I} - \left[\mathbf{K}\mathbf{B} \otimes \mathbf{K}\mathbf{B}\right]\right)^{-1} \left[\mathbf{K} \otimes \mathbf{K}\right] \mathcal{E}\left[\mathbf{G}_t \otimes \mathbf{G}_t\right]\left[\mathbf{u} \otimes \mathbf{u}\right]. \tag{S52}$$

**Segue about K**

Recall the projection operator $\mathbf{P} = \mathbf{u}\mathbf{v}^T$ in equation (S2) and the decomposition $\mathbf{B} = \mathbf{P} + \mathbf{Q}$

in equation (S4). Note that $\mathbf{P}$ and $\mathbf{Q}$ are orthogonal ($\mathbf{PQ} = 0$). Using these,

$$\mathbf{Pu} = \mathbf{u}, \tag{S53}$$

$$\mathbf{e}^T\mathbf{P} = \mathbf{v}^T, \tag{S54}$$

$$\mathbf{ue}^T\mathbf{P} = \mathbf{P}, \tag{S55}$$

$$\mathbf{PK} = \mathbf{P} - \mathbf{u}\,\mathbf{e}^T, \tag{S56}$$

$$\mathbf{QK} = \mathbf{Q}, \tag{S57}$$

$$\mathbf{BK} = \mathbf{P} - \mathbf{u}\,\mathbf{e}^T + \mathbf{Q} = \mathbf{B} - \mathbf{ue}^T \tag{S58}$$

$$\mathbf{KB} = \mathbf{KP} + \mathbf{KQ} = \mathbf{KQ}, \tag{S59}$$

$$\mathbf{K}^n = \mathbf{K}, n \geq 2, \tag{S60}$$

$$[\mathbf{KQ}]^2 = \mathbf{KQKQ} = \mathbf{KQ}^2. \tag{S61}$$

Finally, for completeness, we return to equation (S52) and show that the strange looking Kronecker product converges:

$$[\mathbf{I} - (\mathbf{KB} \otimes \mathbf{KB})]^{-1} = \mathbf{I} + \mathbf{KB} \otimes \mathbf{KB} + (\mathbf{KB} \otimes \mathbf{KB})^2 + \ldots, \tag{S62}$$

$$(\mathbf{KB} \otimes \mathbf{KB})^2 = [\mathbf{KB} \otimes \mathbf{KB}]\,[\mathbf{KB} \otimes \mathbf{KB}]\,, \tag{S63}$$

$$= (\mathbf{KB})^2 \otimes (\mathbf{KB})^2, \tag{S64}$$

$$= (\mathbf{KQ}^2) \otimes (\mathbf{KQ}^2), \tag{S65}$$

$$= (\mathbf{K} \otimes \mathbf{K})\,(\mathbf{Q}^2 \otimes \mathbf{Q}^2). \tag{S66}$$

The point here is that the Kronecker product inverse inherits convergence from the powers of $\mathbf{Q}$. Recall equation (S6) and comments after. So the var-cov of $\mathbf{z}_t$ will be larger if convergence is slower, i.e., will rise with $T_c$.

**Back to the derivation of Var($\Delta_Z$)**

From equation (S49) we have

$$\mathcal{E}\left[(\mathbf{e}^T\mathbf{B}\mathbf{z}_{t-1})^2\right] = \left(\mathbf{e}^T \otimes \mathbf{e}^T\right)\,(\mathbf{B} \otimes \mathbf{B})\,\mathcal{E}\left[\mathbf{z}_t \otimes \mathbf{z}_t\right]. \tag{S67}$$

And we have the var-cov of $\mathbf{z}_t$ from equation (S52).

Therefore, finally, the variance of $\Delta_Z$ is:

$$\mathrm{Var}(\Delta_Z) = \lambda_d^2 \, \mathcal{E}[(\mathbf{e}^T \mathbf{B} \mathbf{z}_{t-1})^2] \tag{S68}$$

$$\boxed{\mathrm{Var}(\Delta_Z) = \lambda_d^2 \left(\mathbf{e}^T \otimes \mathbf{e}^T\right) (\mathbf{B} \otimes \mathbf{B}) \, \mathcal{E}\left[\mathbf{z}_t \otimes \mathbf{z}_t\right]} \tag{S69}$$

Predictions:

a) The size of fluctuations (in $\mathbf{H}_t$ and thus $\mathbf{G}_t$) affects the fluctuations in $\mathbf{z}_t$ and will carry through to fluctuations in $\lambda_t$.

b) Previous work shows that convergence (powers of $\mathbf{Q}$ going to zero) is related to generation time (Jaggi et al., 2026; Jiang et al., 2022). Based on that, we can expect that species with a high generation time will show higher contributions from $\Delta_Z$ because of increase in $\mathcal{E}\left[\mathbf{z}_t \otimes \mathbf{z}_t\right]$.

If the environmental sequence is temporally correlated, there will be additional terms due to interaction between $\mathbf{z}_{t-1}$ and $\mathbf{G}_t\mathbf{u}$ and in that case the full decomposition for the variance expression should be used as shown in equation (S42).

## S6 Simulation procedure

To numerically calculate the terms in the decomposition of variance in population growth rate into the terms shown in Equation (S43), we use a simulation procedure wherein we generate a large number of replicate population trajectories. For each simulated trajectory, we use an initial population vector that is evenly distributed across classes. To remove any effects of this initial population vector, we use a burn-in period, *i.e.*, simulation time steps that are discarded before calculating the decomposition. The decomposition is then calculated for one time step following the burn-in.

(1) We select a population represented by $m$ annual transition matrices (*e.g.*, same grassland plot for $m$ different years). In the case studies presented here, we used populations from the COMADRE and COMPADRE databases (Salguero-Gómez et al., 2015; Salguero-Gómez et al., 2016).

(2) We calculate the burn-in time as $100T_g$, where $T_g$ is the generation time of the mean matrix $\overline{\mathbf{A}}$. We calculate the mean survival and fertility matrices by taking the element-wise average of the $m$ $\mathbf{U}$ and $\mathbf{F}$ matrices, and use these mean matrices to calculate the generation time. Here, we used the definition of generation time from Bienvenu and Legendre (2015), *i.e.,* the average age difference between parents and offspring.

(3) For each of $n$ replicate simulations, we generate a sequence of environments of length $t_{burn-in} + 1$. The $m$ annual transition matrices have equal probabilities of being chosen at each time step. We generate this as a $m \times n$ matrix of environments where each column corresponds to one replicate. We refer to the projection matrix for a given time step $t$ in the environmental sequence for a given replicate $i$ as $\mathbf{A}_{i,t}$.

(4) Because our replicates are a finite sample of matrices, we need to correct for the sample mean in the final time step. In other words, it takes an extremely large number of replicate runs to ensure that the mean (across replicates) of the final-time-step $\mathbf{A}_{i,t_{final}}$ matrices would exactly match $\overline{\mathbf{A}}$. To correct for this, we calculate the offset in matrix elements between $\overline{\mathbf{A}}$ and our sample mean, and add this offset to our sampled final-time-step matrices $\mathbf{A}_{i,t_{final}}$.

(5) For each replicate run $i$:

- We run the burn-in time steps, starting from a population with $1/s$ individuals in each size (or stage, or age) class, where $s$ is the number of size (or stage, or age) classes. For each time $t$, we evaluate $\mathbf{A}_{i,t}\mathbf{w}_{t-1}$. After each iteration, we re-normalize the population vector to the population structure ($\mathbf{w}_t$, where the sum of entries is equal to 1). Because the vital rates are not dependent on population size or density, it is only the relative size of the different size (or stage, or age) classes that matters for driving variation in population growth rate. Therefore, since we are not concerned with the total population size, we re-normalize the population vectors at each time step. This re-normalization avoids numerical errors related to storing large numbers in computing languages such as R.
- For the final time step, we save the environmental matrix ($\mathbf{A}_{i,t_{final}}$), the population structure at the start of the final time step ($\mathbf{w}_{i,t-1}$), and the one-time-step population growth rate ($\lambda_{i,t} = \|\mathbf{w}_{i,t}\|_1 / \|\mathbf{w}_{i,t-1}\|_1$).

(6) After all the replicate simulations are run, we have $n$ realizations of $\lambda_t$, for which we can calculate $\Delta_Z$, $\Delta_R$, and $\Delta_{ZR}$ according to Equation (4) in the main text. Then we calculate the variances and covariances as given in Equation (5).